Organic Process
Research & Development

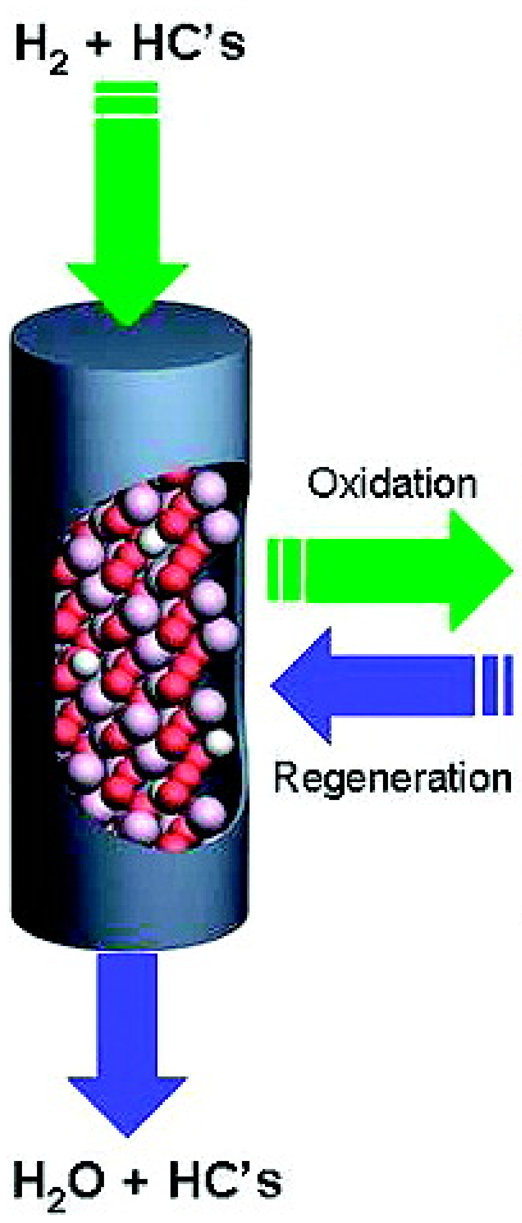

Organic Process Research & Development is published by the American Chemical Society. 1155 Sixteenth Street N.W., Washington, DC 20036

Organic Process
Research & Development

Organic Process Research & Development is published by the American Chemical Society. 1155 Sixteenth Street N.W., Washington, DC 20036

Organic Process Research & Development **2005**, *9,* 397–403

Full Papers

Two-Step Catalytic Oxidative Dehydrogenation of Propane: An Alternative Route to Propene

E. A. de Graaf, G. Zwanenburg,* G. Rothenberg,[†] and A. Bliek[‡]

Van't Hoff Institute for Molecular Sciences, University of Amsterdam, Nieuwe Achtergracht 166, 1018 WV Amsterdam, The Netherlands, and Twente University, P.O. Box 217, 7500 AE Enschede, The Netherlands

Abstract:

The use of solid oxygen carriers (SOCs) in catalytic dehydrogenation may provide a more efficient production process for small alkenes by shifting the equilibrium to the product side. In this paper we use dynamic simulations to investigate the feasibility of two-step oxidative dehydrogenation of propane to propene using a SOC. The proposed process is carried out in a cyclically operated fixed-bed reactor, filled with a mixture of a dehydrogenation catalyst and a SOC. In the first step (the dehydrogenation), propane is fed to the reactor. The SOC oxidises the hydrogen produced during the dehydrogenation. In the second step, the SOC is regenerated and the accumulated coke burned off by allowing oxygen into the reactor. We determine the cyclic steady states by simulating the process for different feed temperatures and SOC concentrations, and we show that addition of a SOC to a reactor filled with dehydrogenation catalyst increases the conversion of propane and enhances the selectivity towards propene.

Introduction

Ethene, propene, and (iso)butene are the primary skeletal building blocks for numerous polymers and are used in various industrial processes. Correspondingly, industrial supply and demand for these alkenes is huge, making low production cost and high production efficiency of large commercial interest. At present there are two main routes to produce propene on an industrial scale. The (hydro)thermal or catalytic cracking of alkanes and naphthas[9,27] and the catalytic dehydrogenation of alkanes, usually employing a platinum or chromium oxide catalyst on alumina.[2,28]

Catalytic cracking gives many by-products and is not necessarily optimized with respect to propene yield. Propane dehydrogenation, on the other hand, yields propene as the

---

* Author for correspondence. E-mail: g.zwanenburg@uva.nl.

[†] University of Amsterdam.

[‡] Twente University.

(1) Barin, I., Ed. *Thermochemical Data of Pure Substances, Part 1*; VCH: Weinheim, Germany, 1989.

(2) Bhasin, M. M.; McCain, J. H.; Vora, B. V.; Ismai, T.; Pujadó, P. R. Dehydrogenation and oxydehydrogenation of paraffins to olefins. *Appl. Catal., A* **2001**, *221*, 397−419.

(3) Caballero, A.; Dexpert, H.; LePeltier, F.; Didillon, B.; Lynch, J. Study by EXAFS and TEM of the effect of the reduction−oxidation cycles over Pt/Al_2O_3-K and PtSn/Al_2O_3-K catalysts. *Jpn. J. Appl. Phys.* **1993**, *32*, 442−444.

(4) Chen, K.; Xie, S.; Bell, A. T.; Iglesia, E. Alkali effects on molybdenum oxide catalysts for the oxidative dehydrogenation of propane. *J. Catal.* **2000**, *195*, 244−252.

(5) Cherian, M.; Rao, M. S.; Hirt, A. M.; Wachs, I. E.; Deo, G. Oxidative Dehydrogenation of propane over supported chromia catalysts: influence of oxide supports and chromia loading. *J. Catal.* **2002**, *211*, 482−495.

(6) Choi, Y.-S.; Park, Y.-K.; Chang, J.-S.; Park, S.-E.; Cheetham, A. K. Oxidative dehydrogenation of 4-vinylcyclohexene into styrene over ZrO_2 catalyst promoted with Fe_2O_3 and CaO. *Catal. Lett.* **2000**, *69*, 93−102.

(7) Courson, C.; Taouk, B.; Bordes, E. Ion oxide conductor as a catalytic membrane for selective oxidation of hydrocarbons. *Catal. Lett.* **2000**, *66*, 129−138.

(8) de Graaf, E. A.; Rothenberg, G.; Kooyman, P. J.; Andreini, A.; Bliek, A. $Pt_{0.02}Sn_{0.003}Mg_{0.06}$ on γ-alumina: a stable catalyst for oxidative dehydrogenation of ethane. *Appl. Catal., A* **2005**, *278*, 187−194.

(9) Gerhartz, W., Ed. *Ullmann's Encyclopedia of Industrial Chemistry*; VCH: Weinheim, 1987; Vol. A10.

(10) Grasselli, R. K.; Stern, D. L.; Tsikoyiannis, J. G. Hydrogen combustion (SHC): II. DH+SHC catalysts physically mixed (redox process mode). *Appl. Catal., A* **1999**, *189*, 9−14.

(11) Grasselli, R. K.; Stern, D. L.; Tsikoyiannis, J. G. Catalytic dehydrogenation (DH) of light paraffins combined with selective hydrogen combustion (SHC). I. DH → SHC → DH catalysts in series (co-fed process mode). *Appl. Catal., A* **1999**, *189*, 1−8.

(12) Julbe, A.; Farrusseng, D.; Cot, D.; Guizard, C. The chemical valve membrane: a new concept for an auto-regulation of O_2 distribution in membrane reactors. *Catal. Today* **2001**, *67*, 139−149.

(13) Kodde, A.; Fokma, Y. S.; Bliek, A. Selectivity effects on series reactions by reactant storage and PSA operation. *AIChE J.* **2000**, *46*, 2295−2304.

(14) Lin, C. H.; Lee, K. C.; Wan, B. Z. Development of catalyst system for selective combustion of hydrogen. *Appl. Catal., A* **1997**, *164*, 59−67.

(15) Moriceau, P.; Grzybowska, B.; Barbaux, Y.; Wrobel, G.; Hecquet, C. Oxidative dehydrogenation of isobutane on Cr−Ce−O oxide: I. Effect of the preparation method and of the Cr content. *Appl. Catal. A General* **1998**, *168*, 269−277.

(16) Park, S.; Vohs, J. M.; Gorte, R. J. Direct oxidation of hydrocarbons in a solid-oxyde fuel cell. *Nature* **2000**, *404*, 265−267.

(17) Patankar, Z. V. *Numerical heat transfer and fluid flow*; McGraw-Hill Book Company: New York, 1980.

(18) Pedernera, M.; Alfonso, M. J.; Menendez, M.; Santamaria, J. Simulation of a catalytic membrane reactor for the oxidative dehydrogenation of butane. *Chem. Eng. Sci.* **2002**, *57*, 2531−2544.

(19) Reid, R. C.; Prausnitz, J. M.; Poling, B. E. *The properties of gases and liquids*, 4th ed.; McGraw-Hill Book Company: New York, 1988.

(20) Rothenberg, G.; de Graaf, E. A.; Bliek, A. Solvent-Free Synthesis of Rechargeable Solid Oxygen Reservoirs for Clean Hydrogen Oxidation. *Angew. Chem., Int. Ed.* **2003**, *42*, 3365−3369.

(21) She, Y.; Han, J.; Ma, Y. H. Palladium membrane reactor for the dehydrogenation of ethylbenzene to styrene. *Catal. Today* **2001**, *67*, 43−53.

(22) Sheintuch, M.; Dessau, R. M. Observations, modelling and optimization of yield, selectivity and activity during dehydrogenation of isobutane and propane in a Pd membrane reactor. *Chem. Eng. Sci.* **1996**, *51*, 535−547.

(23) Téllez, C.; Abon, M.; Dalmon, J. A.; Mirodatos, C.; Sanamara, J. Oxidative dehydrogenation of butane over VMgO catalysts. *J. Catal.* **2000**, *195*, 113−124.

(24) van der Zande, L. M.; de Graaf, E. A.; Rothenberg, G. Design and parallel synthesis of novel selective hydrogen oxidation catalysts and their application in alkane dehydrogenation. *Adv. Synth. Catal.* **2002**, *344*, 884−889.

10.1021/op050020r CCC: $30.25 © 2005 American Chemical Society
Published on Web 05/20/2005

main product. The problem is that the dehydrogenation equilibrium favors propene only at high temperature or low pressure, adding to the overall cost of the process. The need for cryogenic separation of the unconverted propane and produced propene also adds to the process costs. Improvements of the dehydrogenation process to make it commercially more attractive focus on increasing the yield by shifting the equilibrium through removal of one of the reaction products. Thus, in situ removal of hydrogen will shift the dehydrogenation equilibrium to the product side. This can be done either physically by means of a membrane[21,22,29] or chemically by in situ catalytic oxidation using a (post) transition metal or its oxide.[4−6,10,14,15,23] The latter approach has the additional advantage of energy release by exothermic oxidation where it is needed to aid the dehydrogenation. However, mixing oxygen, hydrogen, and hydrocarbons at high temperatures creates a highly dangerous mixture. The risk of explosion may be reduced by separating the reactants in space using dense ion-conducting oxide[7,16] or oxygen-selective membranes.[12,18]

Recently, we demonstrated a novel two-step process for the dehydrogenation of small alkanes.[20] We used a solid oxygen carrier (SOC)[11,24] to selectively remove hydrogen from the reactor to improve product yield. Following depletion of the SOC, oxygen is admitted in the second step to reoxidise the SOC. The SOC is typically a metal oxide that can be easily reduced by hydrogen and reoxidized by oxygen. Depending on the choice of SOC, the reduction by hydrogen can be endothermic (e.g. deep reduction of CeO_2 to Ce_2O_3) or exothermic (e.g. Fe_3O_4 to FeO)[1]. Exothermic reduction gives the energy gain immediately to support the endothermic dehydrogenation of the alkane. When the reduction is endothermic, heat is released during the reoxidation step of the SOC and stored in the catalyst bed to be carried over to the next cycle. Our top SOC, $Ce_{0.9}W_{0.1}O_x$, gave a >97% selectivity to hydrogen oxidation under laboratory conditions. This material could, when coupled to a thermally stable dehydrogenation catalyst,[8] form the basis for a new oxidative dehydrogenation process. The question is: Will selective removal of hydrogen by a SOC in a two-step dehydrogenation process improve conversion and selectivity in a real reactor? In this paper, we present the results of calculations of a simulated reactor running our proposed two-step oxidative dehydrogenation of propane, showing that the process is feasible for a SOC with an endothermic reduction.

The Two-Step Propane Dehydrogenation Process. The two-step oxidative dehydrogenation of propane we propose takes place in a fixed-bed reactor filled with a homogeneous mixture of a dehydrogenation catalyst and a SOC (see Figure 1). During the first step, propane reacts in the following processes: homogeneous and heterogeneous dehydrogenation, eq 1, homogeneous cracking, eq 2, and homogeneous and heterogeneous hydrogenolysis, eqs 3 and 4. For the dehydrogenation reaction we selected a conventional platinum-based dehydrogenation catalyst as described by van Sint Annaland et al.[25,26]

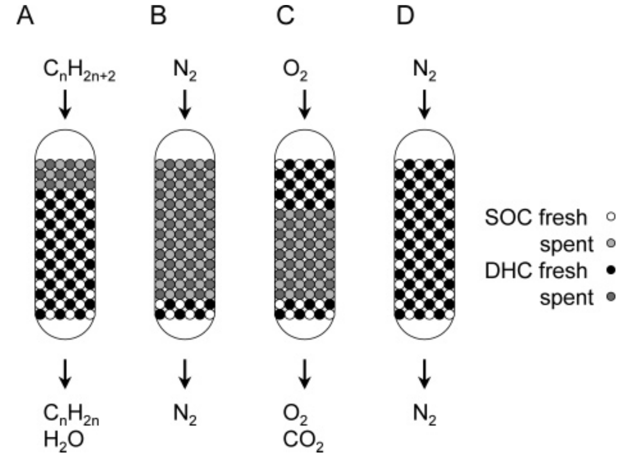

Figure 1. **Reactor configuration: a fixed bed is filled with SOC and dehydrogenation catalyst. A nitrogen-diluted propane feed is fed to the bed (A). Before the break-through the bed is purged with inert nitrogen (B). The bed is regenerated with nitrogen-diluted oxygen: the SOC is replenished, and the coke is burned off (C). After purging with inert nitrogen the bed is ready for dehydrogenation again (D).**

$$C_3H_8 \leftrightarrow C_3H_6 + H_2 \tag{1}$$

$$C_3H_8 \rightarrow C_2H_4 + CH_4 \tag{2}$$

$$C_3H_8 + H_2 \rightarrow C_2H_6 + CH_4 \tag{3}$$

$$C_3H_6 + H_2 \rightarrow C_2H_4 + CH_4 \tag{4}$$

The dehydrogenation catalyst suffers from the formation of coke, especially at the elevated temperatures at which the dehydrogenation reaction takes place. In our model we incorporate the coke formation from a propene precursor (eq 5). We will assume that the coke consists of carbon only.

$$C_3H_6 \rightarrow 3C + 3H_2 \tag{5}$$

To prevent the hydrogen from reacting back with propene, the hydrogen is converted to water at a SOC, eq 6. In our simulations we consider an idealized SOC[20] which is assumed to oxidise hydrogen instantaneously with 100% selectivity.

$$2CeO_2 + H_2 \rightarrow Ce_2O_3 + H_2O \tag{6}$$

After a certain time on-stream the SOC becomes depleted, and the activity of the dehydrogenation catalyst is hampered by coke formation. The reactor is then purged with nitrogen to prevent the formation of flammable or explosive mixtures. In the second step the reactor is reoxidized with a 99:1 v/v N_2:O_2 mixture. The dehydrogenation catalyst is burned clean from coke, and the SOC is replenished. In the simulations

---

(25) van Sint Annaland, M. A novel reverse flow reactor coupling endothermic and exothermic reactions. Ph.D. Thesis, Twente University, 2000.

(26) van Sint Annaland, M.; Kuipers, J. A. M.; van Swaaij, W. P. M. A kinetic rate expression for the time-dependent coke formation rate during propane dehydrogenation over a platinum alumina monolith catalyst. *Catal. Today* **2001**, *66*, 427−436.

(27) Waddams, A. L. *Chemicals from Petroleum*; John Murray: London, 1978.

(28) Weckhuysen, B. M.; Schoonheydt, R. A. Alkane dehydrogenation over supported chromium oxide catalysts. *Catal. Today* **1999**, *51*, 223−232.

(29) Ziaka, Z. D.; Minet, R. G.; Tsotsis, T. T. A high-temperature catalytic membrane reactor for propane dehydrogenation. *J. Membr. Sci.* **1993**, *77*, 221−225.

Table 1. **Input parameters and variables used in the calculations of the two-step oxidative dehydrogenation**

symbol	name	value	unit
ΔH	reaction enthalpy	variable	J mol $^{-1}$
ϵ	void fraction of the bed	0.69	–
λ_{cat}	effective packed bed heat conductivity	0.50	J K^{-1} m^{-1} s^{-1}
μ_{ij}	reaction coefficient homogeneous reaction	–	–
ν_{ij}	reaction coefficient heterogeneous reaction	–	–
ρ	molar density	variable	mol m^{-3}
ρ_{cat}	mass density of SOC/ dehydrogenation catalyst	4×10^3	kg m^{-3}
a	external surface area	2500	m^2 m^{-3}
$C_{\mathrm{p,cat}}$	heat capacity catalyst	1160	J K^{-1} kg^{-1}
$C_{\mathrm{p,gas}}$	heat capacity gas	variable	J K^{-1} mol^{-1}
D_{ax}	axial dispersion coefficient	10^{-5}	m^2 s^{-1}
F	molar flow	variable	mol m^{-2} s^{-1}
h_f	heat transfer coefficient	200	J K^{-1} m^{-2} s^{-1}
k_l	mass transfer coefficient	10^{-3}	m s^{-1}
L	reactor length	5	m
R_i	reaction rate of reaction i	variable	mol m^{-2} s^{-1}
S_{BET}	catalyst surface area	1.53×10^4	m^2 kg^{-1}
t	time coordinate	variable	s
T	temperature of the gas phase	variable	K
T_{s}	temperature of the solid phase	variable	K
x	reactor length coordinate	variable	m
Y_i	gas fraction component i	variable	–
$Y_{i,\mathrm{S}}$	gas fraction component i at surface	variable	–

we assume that both the reoxidation of the SOC as well as the combustion of carbon are instantaneous reactions and that coke is removed from the carrier during the oxidation step. After a second purge with nitrogen the reactor is ready for a new cycle.

The Process Model. To study the feasibility of the process described in the previous section, we calculated process variables such as conversion, selectivity, heat formation, and yields using the gPROMS program (gPROMS, version 2.1.1., PSE Enterprise Ltd., London). In our model, we incorporated the reactions described above and studied the reactor performance for a SOC with an endothermic reduction by hydrogen. The reactor consists of a one-dimensional bed filled with a catalyst phase comprising the two different uniformly dispersed active sites: dehydrogenation catalyst sites and solid oxygen carrier sites. The catalyst is treated as a pseudohomogeneous impermeable phase of constant voidage and density. The gas is introduced at one end of the reactor and moves in plug flow with superimposed axial dispersion over the bed. We follow Reid[19] to describe the physical properties of the gas phase using data for the pure components. The pressure drop over the bed and the radial dispersion in concentration and temperature are assumed to be negligible. Diffusion limitation in the catalyst particles is neglected. The diffusional mass balance of this reactor is described by eq 7. The symbols used in the equations are explained in Table 1.

$$\epsilon\frac{\partial(\rho Y_i)}{\partial t} = -\frac{\partial(FY_i)}{\partial x} + \epsilon\frac{\partial}{\partial x}\left(\rho D_{ax}\frac{\partial Y_i}{\partial x}\right) + \mathrm{N}_{i,\mathrm{SOC}} + \mathrm{N}_{i,\mathrm{DHC}} + \epsilon\sum_k \mu_{i,k}R_k \quad (7)$$

Equation 7 describes the time development of the mass fluxes, ρY_i, of the components i in the reactor as a result of convection, axial dispersion, chemical reactions in the gas phase, and exchange with the catalyst phase. The mass fluxes toward the SOC and dehydrogenation catalyst reaction sites are denoted by $N_{i,\mathrm{SOC}}$ and $N_{i,\mathrm{DHC}}$, respectively. The concentration of the components at the catalyst surface depends on the type of the site; the dehydrogenation site is a source for hydrogen, whereas the SOC site is a sink (see Figure 2). The molar flux, N_i, of component i is thus a sum of the convection of component i from or to the surface and the mass transfer due to concentration differences of the gas at the solid and in the bulk, eq 8.

$$N_i = \sum_j \nu_{i,j}R_j = k_l a\rho(Y_{i,\mathrm{S}} - Y_i) + Y_{i,\mathrm{S}}\sum_i N_i \quad (8)$$

The mass transfer coefficient of the components, k_l, from the solid to the gas phase is assumed to be constant, with zero accumulation of components on the catalyst phase. Danckwerts-type boundary conditions are applied at the boundaries of the bed.

The heat balance of the reactor is captured in eqs 9 and 10. Equation 9 describes the temperature evolution in the reactor in the gas phase,

$$\epsilon\rho C_{\mathrm{p,gas}}\frac{\partial T}{\partial t} = -FC_{\mathrm{p,gas}}\frac{\partial T}{\partial x} + \epsilon\frac{\partial}{\partial x}\left(\lambda_{\mathrm{gas}}\frac{\partial T}{\partial x}\right) + ah_f(T_{\mathrm{s}} - T) + \epsilon\sum_i\sum_k \mu_{i,k}R_k\Delta H_R \quad (9)$$

and eq 10 describes the development of temperature in the solid phase.

$$(1-\epsilon)\rho_{\mathrm{cat}}C_{\mathrm{p,cat}}\frac{\partial T_{\mathrm{s}}}{\partial t} = ah_f(T - T_{\mathrm{s}}) + (1-\epsilon)\frac{\partial}{\partial x}\left(\lambda_{\mathrm{cat}}\frac{\partial T_{\mathrm{s}}}{\partial x}\right) + \sum_i\sum_j \nu_{i,j}R_j\Delta H_{\mathrm{R}} \quad (10)$$

Table 1 summarises the simulation variables and constants, together with their values and units.

Simulations. We calculated the conversion of propane and determined the selectivity of the reactor towards propene by integrating the mass and heat balances (eqs 7−10) taking into account the dehydrogenation, hydrogenolysis, and cracking of propane and hydrogenolysis of propene in both the gas phase and on the dehydrogenation sites of the solid phase. For these reactions, as well as for the coke-formation process, we used the kinetics data as published by van Sint Annaland et al.[25,26]

The integration was carried out using the gPROMS environment in the form of a second-order upwind scheme.[13] The reactor was discretised based on a staggered grid using 50 cells of equal volume.[17] Component fluxes and velocities were defined at the borders of the cells. Physical properties

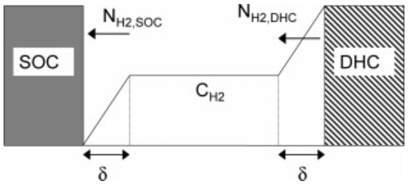

Figure 2. **Schematic concentration profile with dehydrogenation catalyst, gas bulk and SOC. Hydrogen (C_{H_2}, black line) is produced on the dehydrogenation catalyst (DHC) by dehydrogenation. The catalyst surface is separated from the gas bulk by a film with thickness δ. At the surface of the SOC hydrogen is instantaneously oxidised to water. The direction of the $N_{H_2,DHC}$ and $N_{H_2,SOC}$ is presented by arrows (to and from the bulk of the gas).**

such as pressure and temperature were defined at the centers of the cells. The initial bed temperature was taken to be equal to the gas inlet temperature. The latter was kept constant throughout the cycle. The process cycle started with the dehydrogenation step, lasting 600 s with a gas flow of 2 mol m^{-2} s^{-1}, followed by a nitrogen purge for 100 s at a flow rate of 2 mol m^{-2} s^{-1}. For the reoxidation a mixture of 1% oxygen in nitrogen was used at a flow rate of 20 mol m^{-2} s^{-1}. The reoxidation time was taken to be variable to allow time for the coke, formed during the dehydrogenation, to be burned off and the SOC to be replenished. Finally, the reactor was purged again for 100 s with a 2 mol m^{-2} s^{-1} nitrogen flow.

In our study the reactor length is kept constant. For each temperature and SOC content an optimal reactor length can be found, and of course the residence time in the reactor also depends on temperature. The distribution of the volume ratio of catalyst vs SOC, here taken as uniform throughout the reactor, can also influence the performance. A treatment of these effects is beyond the scope of this paper.

Results and Discussion

We determined the cyclic steady state for a reactor filled with a homogeneous mixture of dehydrogenation catalyst and SOC, by the procedure described above. The ratio between the SOC and dehydrogenation catalyst was varied from 0 to 75% vol. of the catalyst phase. The inlet temperature (constant throughout each process cycle) was taken from $T = 748$ K to $T = 873$ K in steps of 25 K.

Propane Conversion and Selectivity. We studied the conversion of propane and determined the selectivities towards propene, coke, and hydrogenolised products (C_2H_6, C_2H_4, CH_4). The performance of the reactor is determined by a balance between competing reactions: on one hand the conversion of propane into propene, on the other hand the (hydro)cracking of propane and conversion of propene in undesirable products. For low inlet temperatures the conversion of propane to propene is low, but so are the rates of the competing reactions, leading to a high selectivity. At higher temperatures, competing reactions start to influence reactor performance by creating more by-products. Thus, the increase in conversion is accompanied by a decrease in selectivity. This is illustrated in Figure 3 by the dotted line connecting the simulations performed without SOC at various temperatures. Figure 3 also shows that removing hydrogen from the reactor increases both conversion and selectivity. However, for a SOC concentration exceeding 10% vol. of the catalyst phase, the conversion goes down, while the selectivity approaches a plateau. The general shape of the lying U-curves can be understood as follows. Initially, both conversion and selectivity increase when more SOC is added. The conversion increases because the presence of the SOC removes hydrogen, shifting the equilibrium of the dehydrogenation reaction of propane to the product side. The selectivity increases because the removal of hydrogen from the reactor prevents hydrogenolysis reactions from taking place. However, when SOC concentration reaches 10% vol. of the catalyst phase, conversion starts to decrease when the SOC concentration is increased further, while the rise in selectivity is only marginal at best. At this point the diminishing amount of dehydrogenation catalyst is no longer compensated by the shift in equilibrium in favor of the dehydrogenation products. The selectivity no longer increases because most of hydrogen is already oxidized by the SOC. This pattern holds for temperatures up to 798 K. Addition of more than 10% SOC increases the selectivity, but the conversion drops.

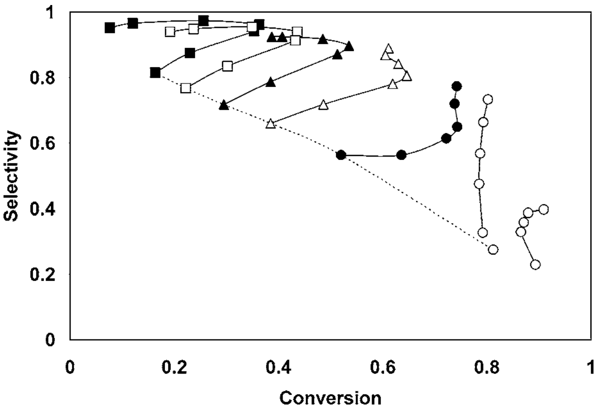

Figure 3. **Selectivity towards propene versus conversion of propane plot of the two-step oxidative dehydrogenation. The entrance temperature of the feed streams is varied: (■) 748 K, (□) 773 K, (▲) 798 K, (△) 823 K, (●) 848 K, and (○) 873 K with double steady state. The SOC content as volume fraction of the bed is varied for each temperature: 0, 1, 5, 10, 25, 50, and 75%, respectively. The 0% SOC points are connected by a dotted line. Lines are used to guide the eye.**

At $T = 823$ K we see a similar pattern for lower SOC concentrations: Adding a small amount of SOC increases conversion and selectivity. The pattern changes when the reactor is filled with 75% vol. SOC. Now selectivity and conversion increase compared to those at 50% vol. SOC. This pattern is repeated at higher temperatures ($T = 848$ and 873 K) and can be explained by a combination of the following factors. First, at higher temperatures the equilibrium of the dehydrogenation reaction shifts towards the product side, and the reaction rate of the dehydrogenation reaction increases, thus offsetting the drop in conversion due to fewer dehydrogenation sites at higher SOC concentrations and lower temperatures. Second, the hydrogen reduction at the SOC is nearly complete at high temperatures, leaving less hydrogen available for hydrogenolysis, thus increasing selectivity.

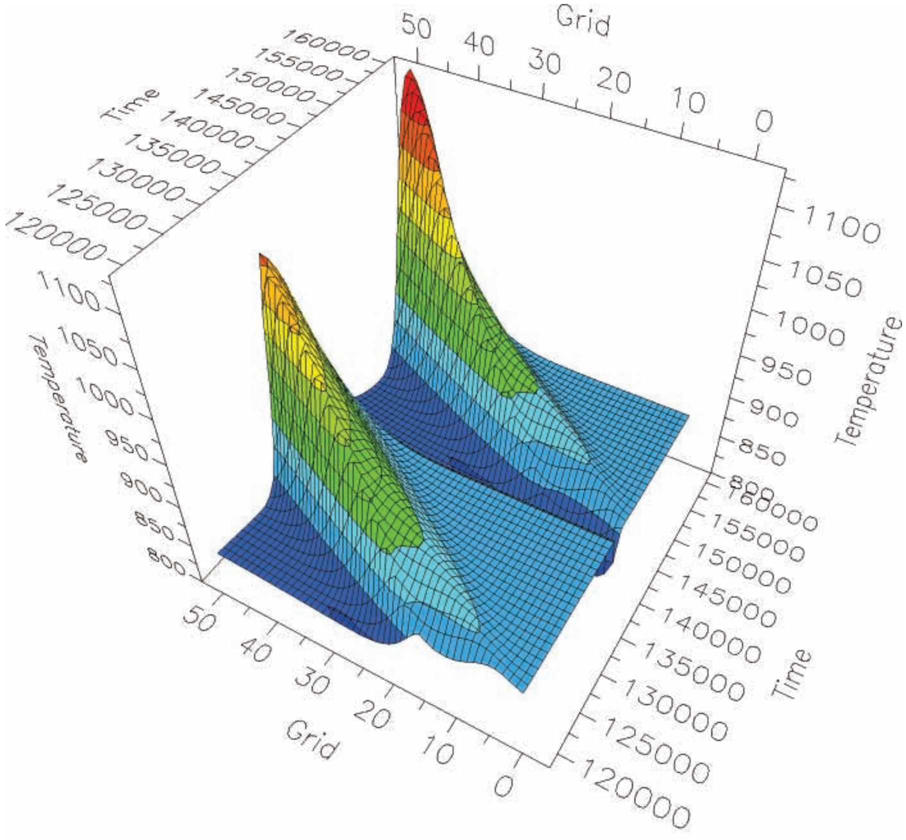

T=873 K; SOC concentration 10%

Figure 4. **Temperature profile of the double cyclic steady state for a reactor filled with a catalyst mixture comprising volume fractions of 10% SOC and 90% dehydrogenation catalyst. The inlet temperature of the gas is 873 K in all four consecutive reaction steps.**

At feed temperatures up to 848 K the reactor has one steady state. Increasing the gas inlet temperature to $T = 873$ K leads to a double steady state (represented in Figure 3 by two series of points at $T = 873$ K). The double steady state occurs when the reactor is uniformly filled with a mixture of SOC and dehydrogenation catalyst (Figure 4). When the reactor is filled with just the dehydrogenation catalyst (SOC concentration 0%), no double steady state is observed. The doubling of the steady state is caused by large temperature swings in the reactor. The first cycle starts with a nearly uniform bed temperature, the temperature of the feed in the oxidation step. Because of the high inlet temperature, a considerable amount of coke is deposited on the bed during the dehydrogenation step. The combustion of this coke in the reoxidation phase generates a considerable temperature rise. At the start of a new cycle, the bed temperature is still high due to the coke burn-off in the previous reoxidation, and large amounts of coke are formed. These large amounts of coke require increasingly long oxidation times. Since the SOC reoxidation and coke burn off are considered instantaneous, a sharp reaction front travels through the reactor. Regenerated parts of the bed have now time to be cooled by the oxidative flow; when all coke is removed and the SOC is replenished in the second cycle, the bed temperature is nearly uniform again.

Hydrogen Conversion and Selectivity. Hydrogen is produced by dehydrogenation and during coke formation. It is consumed by reduction of the SOC or by hydrogenolysis. Even when no SOC is present, hydrogen will be chemically removed by hydrogenolysis. However, hydrogenolysis can destroy the reactant, propane, and the product, propene. Therefore, oxidation of hydrogen can improve propene selectivity by quenching hydrogenolysis. Figure 5 shows the selectivity towards hydrogen oxidation versus the total hydrogen consumption. An increase in the SOC concentration in the reactor increases both the conversion of hydrogen and its selectivity towards water at all temperatures by opening up a reaction path to the oxidation of hydrogen to form water. Adding even a small fraction SOC to the reactor filled with only dehydrogenation catalyst increases the hydrogen conversion significantly (see Figure 6). This supports the phenomena we described before: the addition of only 10% vol. SOC boosts hydrogen conversion to levels higher than 90%. However, an even more efficient hydrogen removal has to compete with the loss of a large amount of dehydrogenation sites.

The reaction rates for the two hydrogen conversion routes are different. Hydrogen is oxidized instantaneously on the SOC, whereas the hydrogenolysis can be described by an Arrhenius-type relation. Figure 6 shows that the hydrogen conversion decreases with increasing temperature. This seems contradictory, since the hydrogen removal rate increases concomitant with temperature. At the same time, however, hydrogen production also increases. The increase is due to

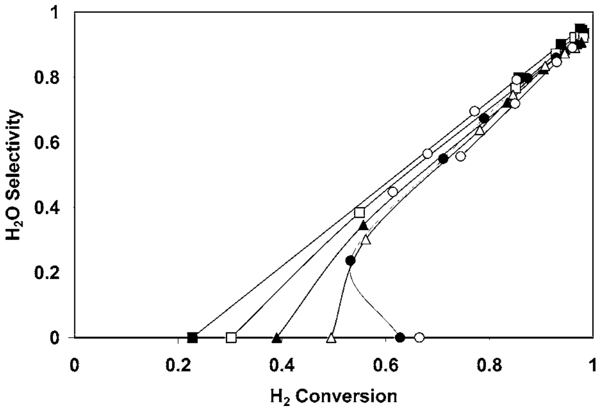

Figure 5. **Selectivity towards water (instead of towards hydrogenolysis products) versus conversion (ratio between the reacted and formed hydrogen) plot of the hydrogen consumption. The entrance temperature of the feed streams is varied: (■) 748 K, (□) 773 K, (▲) 798 K, (△) 823 K, (●) 848 K, and (○) 873 K with double steady state. For each temperature the points indicate the SOC content as volume fraction of the bed: 0, 1, 5, 10, 25, 50, and 75%, respectively. Lines are used to guide the eye.**

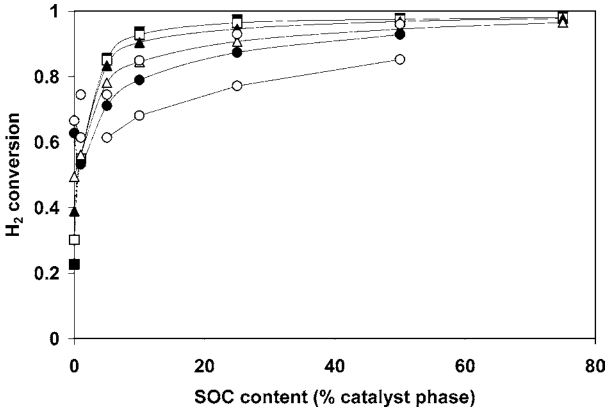

Figure 6. **Hydrogen conversion versus SOC content in the fixed bed. The entrance temperature of the feed streams is varied: (■) 748 K, (□) 773 K, (▲) 798 K, (△) 823 K, (●) 848 K, and (○) 873 K with double steady state. For each temperature the SOC content as volume fraction of the bed is varied: 0, 1, 5, 10, 25, 50, and 75%, respectively. Lines are used to guide the eye.**

the shift in reaction equilibrium of propane dehydrogenation towards the product side and to a strong increase in coke formation (with associated hydrogen production). Thus, although more hydrogen is removed, even more is formed at high temperatures, explaining the overall lower hydrogen conversion.

Propene Productivity vs Selectivity. Coke combustion and reoxidation of the SOC both require large amounts of oxygen. This leads to long reoxidation times, especially for high inlet temperatures. The total cycle time can lengthen to up to 75 times the time required for the dehydrogenation step. This means that high conversions do not automatically lead to high production rates (defined as propene yield divided by cycle time). Figure 7 shows the selectivities versus production rate. At a first glance, the results seem contrary to those presented in Figure 3—the highest production rates are obtained at the lowest inlet temperatures. However, at higher inlet temperatures more coke is formed, which takes more time to burn off. Roughly 50% of the oxygen in the reoxidation step goes to coke burning instead of reoxidizing the solid oxygen carrier. This leads to longer cycle times and lower production rates.

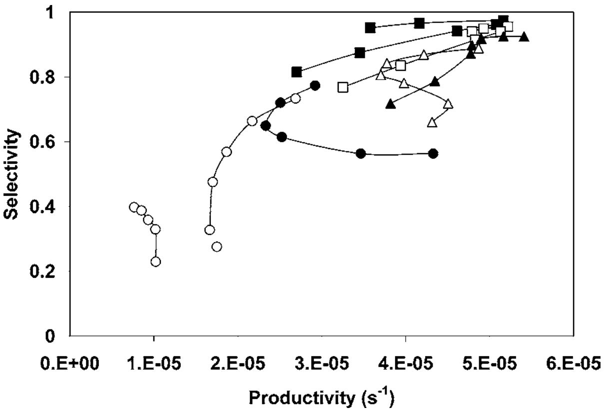

Figure 7. **Selectivity versus yield/cycle time plot of the two-step oxidative dehydrogenation. The entrance temperature of the feed streams is varied: (■) 748 K, (□) 773 K, (▲) 798 K, (△) 823 K, (●) 848 K, and (○) 873 K with double steady state. The volume fraction SOC of the bed is varied for each temperature: 0, 1, 5, 10, 25, 50, and 75%, respectively. Lines are used to guide the eye.**

Alternative Oxidants: Pros and Cons. Reoxidation times of the two-step oxidative dehydrogenation process are extensive, especially when the reactor is operated at elevated temperatures. One option to shorten the cycle time is to increase the oxygen content of the oxidizing feed stream. However, this will destroy the platinum dispersion on the catalyst[3] and will also lead to a large temperature rise in the bed. A better alternative is using high concentrations of milder oxidants, for example CO_2 or H_2O to replenish the SOC. If these mild oxidants would not be sufficient to burn of the coke, a further oxidation step with oxygen can be applied after the mild reoxidation step. Because the SOC is already replenished, significantly less time will be required for this oxidation step.

H_2O is an interesting alternative oxidant because of the hydrogen produced in its reduction. Now the reactor would function as a separator: The hydrogen produced in the dehydrogenation reaction is released in the reoxidation step when H_2O is reduced. Since the reaction with hydrogen is assumed to be instantaneous, oxygen vacancies will concentrate near the exit of the reactor when water is used as oxidant. Only then water can reoxidize the SOC, and the produced hydrogen has a chance to escape the reactor without being reoxidized. When the reduction proceeds at a lower pace than the reoxidation, this process option becomes even more feasible. A drawback for the use of water as oxidant is that the hydrogen production in the reoxidation is endothermic, and thus the energy gained in hydrogen oxidation is lost.

Conclusions

Our results show that the addition of a SOC effectively removes hydrogen produced in the dehydrogenation of propane. This shifts the equilibrium of the dehydrogenation reaction towards the product, propene. Furthermore, that if the SOC is increased to above 10% vol. of the catalyst phase, the benefit of shifting the equilibrium to the propene side by removing hydrogen is overturned by the decrease in conversion due to the diminishing amount of dehydrogenation catalyst. Addition of a SOC in the dehydrogenation of propane increases selectivity and conversion to the desired propene.

At high temperatures, formation of coke increases the cycle time of the reactor significantly due to the longer regeneration times. This negatively affects the production of propene by wasting valuable reactor time in the coke-burning process. As a solution to the long cycle times, we suggest the use of milder oxidants, such as water, in the reoxidation step. Further studies of the use of alternative, milder oxidants to reduce cycle times and to recover hydrogen may suggest ways to further enhance the efficiency and potential of the two-step catalytic dehydrogenation process and will be carried out in our laboratory.

Acknowledgment

E.A.G. gratefully acknowledges financial support from NWO-Chemische Wetenschappen. We thank Process System Enterprise Ltd. for help with implementation of the model in gPROMS and Dr. M. van Sint Annaland for discussions and comments.

Received for review February 15, 2005.

OP050020R